

QCD-Instantons at HERA – An Introduction*

A. Ringwald and F. Schrempp

Deutsches Elektronen-Synchrotron DESY, Hamburg, Germany

Abstract

We review our ongoing theoretical and phenomenological study of the discovery potential for instanton-induced DIS events at HERA. Constraints from recent lattice simulations will be exploited and translated into a “fiducial” kinematical region for our predictions of the instanton-induced DIS cross-section.

*Plenary talk at the 3rd UK Phenomenology Workshop on HERA Physics, Sep 20-25, 1998, Durham/UK.

1 Instantons

Non-abelian gauge theories like QCD are known to exhibit a rich vacuum structure. The latter includes *topologically* non-trivial fluctuations of the gauge fields, carrying an integer topological charge Q . The simplest building blocks of topological structure are instantons ($Q = +1$) and anti-instantons ($Q = -1$) which are well-known explicit solutions of the euclidean field equations in four dimensions [1].

Instantons (I) are widely believed to play an important rôle in various *long-distance* aspects [2] of QCD:

First of all, they may provide a solution of the famous $U_A(1)$ problem [3] ($m_{\eta'} \gg m_\eta$), with the corresponding pseudoscalar mass splitting related to the topological susceptibility in the pure gauge theory by the well-known Witten-Veneziano formula [4]. Moreover, a number of authors have attributed a strong connection of instantons with chiral symmetry breaking [5,2] as well as the hadron and glueball spectrum.

However, there are also very important *short-distance* implications [6,7,8,9,10] of QCD instantons to which the present report is devoted:

Instantons are known to induce certain processes which violate *chirality* in accord with the general axial-anomaly relation [3] and which are forbidden in conventional perturbation theory. Of particular interest in this context is the *deep inelastic scattering* (DIS) regime. Here, hard instanton-induced processes may both be *calculated* [8,9,10] within *instanton-perturbation theory* and possibly be *detected experimentally* [7,11,12,13]. As a key feature it has recently been shown [8], that in deep-inelastic scattering (DIS) the generic hard scale Q cuts off instantons with *large size* $\rho \gg Q^{-1}$, over which one has no control theoretically.

Our finalized results [9,10] for inclusive instanton-induced DIS cross-sections are summarized in sections 2 and 4. Their weak residual renormalization-scale dependence is quite remarkable.

As a second main point of this review (section 3), constraints from recent lattice simulations will be exploited [9,14] and translated into a “fiducial” kinematical region for our predictions of the instanton-induced DIS cross-section based on instanton-perturbation theory. In section 5 we discuss the expected event signature and search strategies based on our Monte Carlo generator [11] QCDINS 1.60. Finally (section 6), we briefly address an interesting class of “fireball” events, observed in photoproduction, in the context of instantons and put forward a promising proposal [14] on extending our theoretical predictions beyond the regime of strict instanton perturbation theory.

2 DIS cross-sections in instanton-perturbation theory

In I -perturbation theory one expands the relevant Green’s functions about the known, classical instanton solution $A_\mu = A_\mu^{(I)} + \dots$ instead of the usual (trivial) field configuration $A_\mu^{(0)} = 0$ and obtains a corresponding set of modified Feynman rules. Like in conventional pQCD, the gauge coupling α_s has to be small.

The leading instanton-induced process in the DIS regime of $e^\pm P$ scattering for large photon virtuality Q^2 is illustrated in figure 1. The dashed box emphasizes the so-called instanton-*subprocess* with its own Bjorken variables,

$$Q'^2 = -q'^2 \geq 0; \quad x' = \frac{Q'^2}{2p \cdot q'} \leq 1. \quad (1)$$

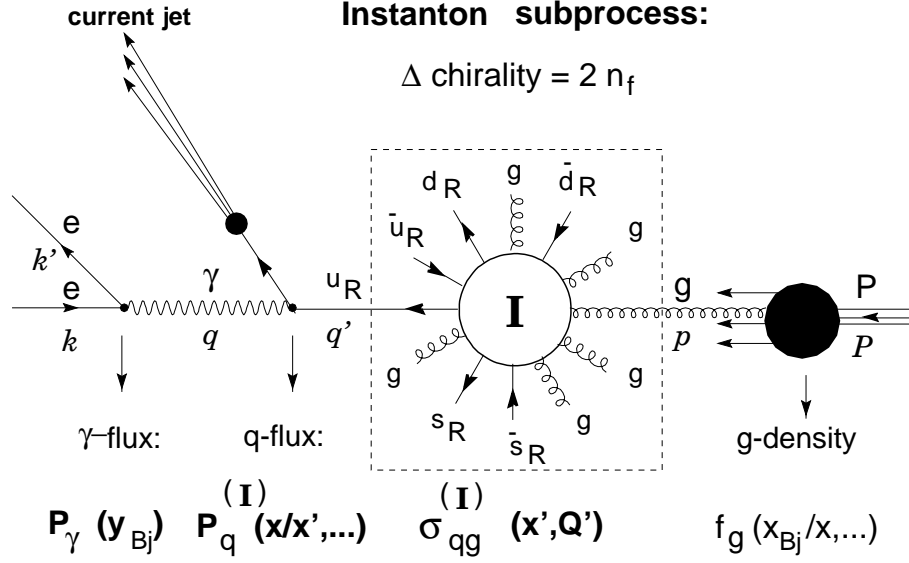


Figure 1: The leading instanton-induced process in the DIS regime of $e^\pm P$ scattering ($n_f = 3$).

It induces a total chirality violation $\Delta \text{chirality} = 2 n_f$, in accord with the corresponding axial anomaly [3]. In the Bjorken limit of I -perturbation theory, the dominant I -induced contribution to the inclusive HERA cross-section may be shown to take the form [9,10]

$$\frac{d\sigma_{\text{HERA}}^{(I)}}{dx'dQ'^2} \simeq \frac{d\mathcal{L}_{qg}^{(I)}}{dx'dQ'^2} \cdot \sigma_{qg}^{(I)}(Q', x'). \quad (2)$$

The differential luminosity, $d\mathcal{L}_{qg}^{(I)}$, accounting for the number of qg collisions per eP collision, has a convolution-like structure. It involves integrations over the gluon density, the γ -flux P_γ and the known q -flux $P_q^{(I)}$ in the I -background (c.f. figure 1). The crucial instanton-dynamics resides in the I -subprocess total cross-section $\sigma_{qg}^{(I)}(Q', x')$, on which we focus our attention next [9,10].

Being an observable, $\sigma_{qg}^{(I)}(Q', x')$ involves integrations over all $I(\bar{I})$ -“collective coordinates”, including the $I(\bar{I})$ -sizes ρ ($\bar{\rho}$) and the $I\bar{I}$ -distance¹ 4-vector R_μ ,

$$\sigma_{qg}^{(I)} = \int_0^\infty d\rho D(\rho) \int_0^\infty d\bar{\rho} D(\bar{\rho}) \int d^4 R \{ \dots \} e^{-Q'(\rho+\bar{\rho})} e^{i(p+q') \cdot R} e^{-\frac{4\pi}{\alpha_s} \Omega\left(\frac{R^2}{\rho\bar{\rho}}, \frac{\bar{\rho}}{\rho}\right)}. \quad (3)$$

The $\rho(\bar{\rho})$ -integrals in (3) involve as generic weight the $I(\bar{I})$ -density $D(\rho(\bar{\rho}))$ [3,15,16],

$$\begin{aligned} D(\rho) &= \frac{d}{\rho^5} \left(\frac{2\pi}{\alpha_s(\mu_r)} \right)^{2N_c} \exp\left(-\frac{2\pi}{\alpha_s(\mu_r)} \right) (\rho \mu_r)^{\beta_0 + \frac{\alpha_s(\mu_r)}{4\pi} (\beta_1 - 4N_c\beta_0)} \\ d &= \frac{2e^{5/6}}{\pi^2 (N_c - 1)!(N_c - 2)!} e^{-1.51137 N_c + 0.29175 n_f} \quad (\overline{\text{MS}} \text{ scheme}); \\ \beta_0 &= \frac{11}{3} N_c - \frac{2}{3} n_f; \quad \beta_1 = \frac{34}{3} N_c^2 - \left(\frac{13}{3} N_c - \frac{1}{N_c} \right) n_f, \end{aligned} \quad (4)$$

with renormalization scale μ_r and $N_c = 3$.

¹Both an instanton and an anti-instanton enter here, since cross sections result from taking the *modulus squared* of an amplitude in the single I background.

The function $\Omega(R^2/(\rho\bar{\rho}), \dots)$ in equation (3), appearing in the exponent with a large numerical coefficient $4\pi/\alpha_s$, incorporates the effects of final-state gluons. Within strict I -perturbation theory, it is given in form of a perturbative expansion [17], while in the so-called $I\bar{I}$ -valley approximation [18,19] Ω is associated with an analytically known closed expression [19,20] for the interaction between I and \bar{I} , $\Omega \simeq \alpha_s/(4\pi)S[A_\mu^{I\bar{I}}] - 1$. With both methods agreeing for larger values of $R^2/(\rho\bar{\rho})$, we have actually used the valley method in our quantitative evaluation.

Due to the nonvanishing virtuality Q'^2 in DIS, the “form factor” $\exp[-Q'(\rho + \bar{\rho})]$ in (3), being associated with the off-shell quark (zero mode) q , suppresses large-size instantons [8,9,10]. Hence, the integrals in (3) are *finite*. In fact, they are dominated by a unique *saddle-point* [9,10],

$$\rho^* = \bar{\rho}^* \sim 1/Q'; \quad R^{*2} \sim 1/(p+q')^2 \Rightarrow \frac{R^*}{\rho^*} \sim \sqrt{\frac{x'}{1-x'}}, \quad (5)$$

from which it becomes apparent that the virtuality Q' controls the effective I -size, while x' determines the effective $I\bar{I}$ -distance (in units of the size ρ).

In figure 2, the resulting I -subprocess cross-sections (3) is displayed [9] over a *large* range of μ_r/Q' for fixed $x' = 0.5$ and $Q'/\Lambda = 30, 50, 70$. Apparently, we have achieved great progress in stability and hence predictivity by using the improved expression (4) of the I -density $D(\rho)$, which is renormalization-group (RG) invariant at the 2 -loop level, i.e. $D^{-1} dD/d\ln(\mu_r) = \mathcal{O}(\alpha_s^2)$. The residual dependence on the renormalization scale μ_r is remarkably flat and turns out to be strongly reduced as compared to the 1-loop case! Throughout, we choose as the “best scale”, $\mu_r = 0.15 Q'$, for which $\partial\sigma_{qg}^{(I)}/\partial\mu_r \simeq 0$ (c.f. figure 2). This choice agrees well with the intuitive expectation [8,6] $\mu_r \sim 1/\langle\rho\rangle \sim Q'/\beta_0 = \mathcal{O}(0.1) Q'$.

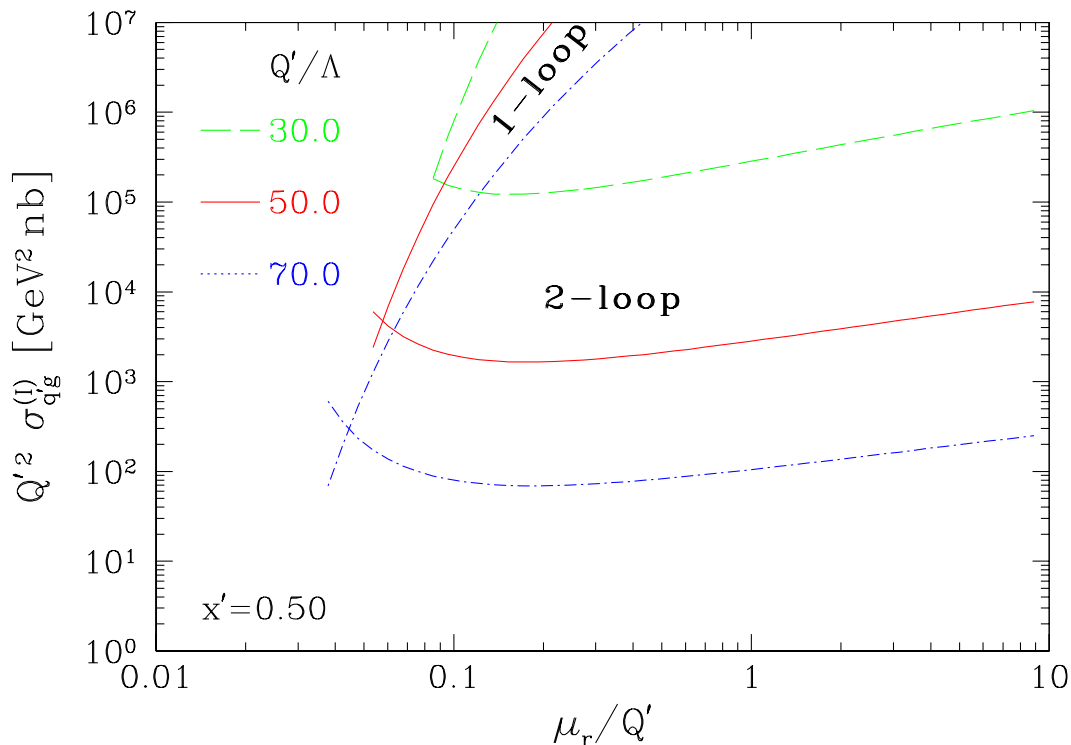


Figure 2: Illustration of the weak residual renormalization-scale (μ_r) dependence of the resulting I -subprocess cross-section $\sigma_{qg}^{(I)}(Q', x')$.

3 “Fiducial” region from lattice simulations

There has been much recent activity in the lattice community to “measure” topological fluctuations in lattice simulations [21] of QCD. Being independent of perturbation theory, such simulations provide “snapshots” of the QCD vacuum including all possible non-perturbative features like instantons (figure 3). Let us discuss next, how these lattice results may be exploited to provide crucial support for the theoretical basis of our calculations in DIS:

To this end, we first perform a *quantitative* confrontation [9,14] of the predictions from I -perturbation theory with a recent high-quality lattice simulation [23] of QCD (without fermions, $n_f = 0$). The striking agreement which we shall find over a range of I -collective coordinates is a very interesting result by itself.

Next, we recall (c.f. (3) and (5)) that the collective coordinate integrals in our DIS cross-section $\sigma_{qg}^{(I)}(Q', x')$ are dominated by a unique, calculable saddle-point $(\rho^*, R^*/\rho^*)$, in one-to-one correspondence to the conjugate momentum variables (Q', x') . This fact then allows us to *translate* the extracted range of validity of I -perturbation theory and the dilute I -gas approximation, $(\rho \leq \rho_{\max}, R/\rho \geq (R/\rho)_{\min})$, directly into a “fiducial” kinematical region $(Q' \geq Q'_{\min}, x' \geq x'_{\min})$ in momentum space!

In lattice simulations 4d-Euclidean space-time is made discrete; specifically, the recent “data” from the UKQCD collaboration [23], which we shall use here, involve a lattice spacing $a = 0.055 - 0.1$ fm and a volume $V = l_{\text{space}}^3 \cdot l_{\text{time}} = [16^3 \cdot 48 - 32^3 \cdot 64] a^4$. In principle, such a lattice allows to study the properties of an ensemble of I 's and \bar{I} 's with sizes $a < \rho < V^{1/4}$. However, in order to make instanton effects visible, a certain “cooling” procedure has to be applied first. It is designed to filter out (dominating) fluctuations of *short* wavelength $\mathcal{O}(a)$ (c.f. figure 3 (a)), while affecting the topological fluctuations of much longer wavelength $\rho \gg a$ comparatively little. After “cooling”, I 's and \bar{I} 's can clearly be seen (and studied) as bumps in the lagrange density and the topological charge density (figure 3 (b), (c)). For a more detailed discussion of lattice-specific caveats, like possible lattice artefacts and the dependence of results on “cooling” etc., see Refs. [21,23].

Of course, one has to extrapolate the lattice observables to the continuum ($a \Rightarrow 0$), before a meaningful comparison with I -perturbation theory can be made. This is complicated by a strong dependence of the various distributions on the number n_{cools} of cooling sweeps for *fixed* $\beta = 6/g_{\text{lat}}^2$.

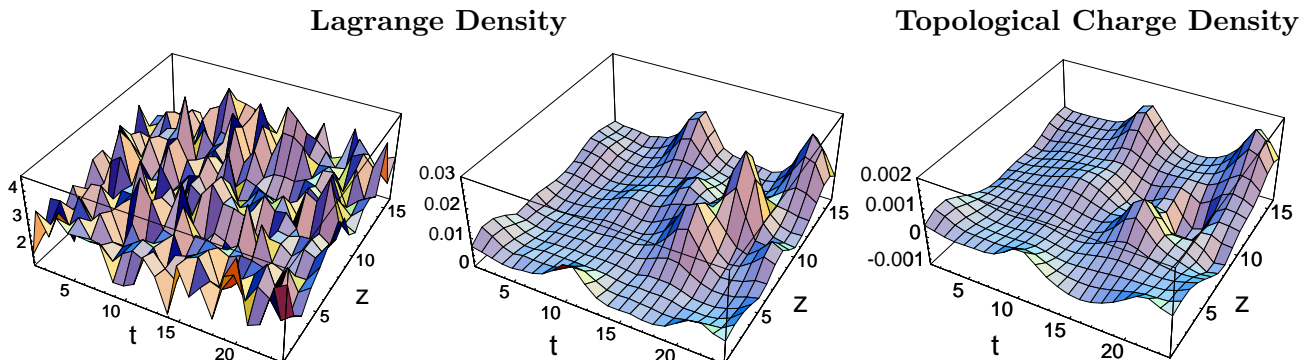


Figure 3: Instanton content of a typical slice of a gluon configuration at fixed x, y as a function of z and t [22]. (a) Lagrange density before “cooling”, with fluctuations of *short* wavelength $\mathcal{O}(a)$ dominating. After “cooling” by 25 steps, 3 I 's and 2 \bar{I} 's may be clearly identified in the lagrange density (b) and the topological charge density (c).

In ref. [23], however, *equivalent* pairs $(\beta, n_{\text{cools}})$ were found, for which *shape* and *normalization* of the distributions essentially remain *invariant*. For instance, the continuum extrapolation of the data for the $(I + \bar{I})$ -density $D_{I+\bar{I}}$ at $(\beta, n_{\text{cools}}) = (6.0, 23)$, $(6.2, 46)$, $(6.4, 80)$, may thus be performed quite reliably [14], by simply rescaling the arguments $\rho \Rightarrow \overline{\rho(0)}/\overline{\rho(a)} \cdot \rho$. Here, $\overline{\rho(0)}$ denotes the continuum limit of the *weakly varying* average ρ values, $\overline{\rho(a)}$, of $D_{I+\bar{I}}(\rho, a)$. A *linear* extrapolation in $(a/r_0)^2$ was employed. For consistency and minimization of uncertainties, one should use only a single dimensionful quantity to relate lattice units and physical units. Throughout our analysis, all dimensions are therefore expressed by the so-called Sommer scale [24, 25] r_0 , with $2r_0 \simeq 1$ fm, which we prefer over the string tension [23]. The resulting “continuum data” for $D_{I+\bar{I}}(\rho)$ are displayed in figure 4. They scale nicely. We are now ready to perform a quantitative comparison with the predictions of I -perturbation theory [14]. For reasons of space, let us concentrate here on the $(I + \bar{I})$ -density $D_{I+\bar{I}}(\rho)$. The prediction (4) of I -perturbation theory is a power law for *small* ρ , i. e. approximately $D \sim \rho^6$ for $n_f = 0$. Due to its 2-loop RG-invariance the normalization of $D_{I+\bar{I}}(\rho)$ is practically independent of the renormalization scale μ_r over a wide range. It is strongly and exclusively dependent on $r_0 \Lambda_{\overline{\text{MS}} n_f=0}$, for which we take the most recent, accurate result by the ALPHA-collaboration [25], $2r_0 \Lambda_{\overline{\text{MS}} n_f=0} = (238 \pm 19)$ MeV fm. In figure 4 (b) we display both this parameter-free prediction from (4) of I -perturbation theory and the continuum limit of the UKQCD data in a log-log plot, to clearly exhibit the expected power law in ρ . The agreement in shape *and* normalization for $\rho \lesssim 0.3 (2r_0) \simeq 0.3$ fm is striking, indeed, notably in view of the often criticized “cooling” procedure and the strong sensitivity to $\Lambda_{\overline{\text{MS}} n_f=0}$.

By a similar analysis [14], we were able to infer from the “equivalent” UKQCD lattice data a range of validity $R/\rho \gtrsim 1$ of the valley expression for the $I\bar{I}$ -interaction $\Omega(R^2/(\rho\bar{\rho}), \dots)$ in (3). Finally,

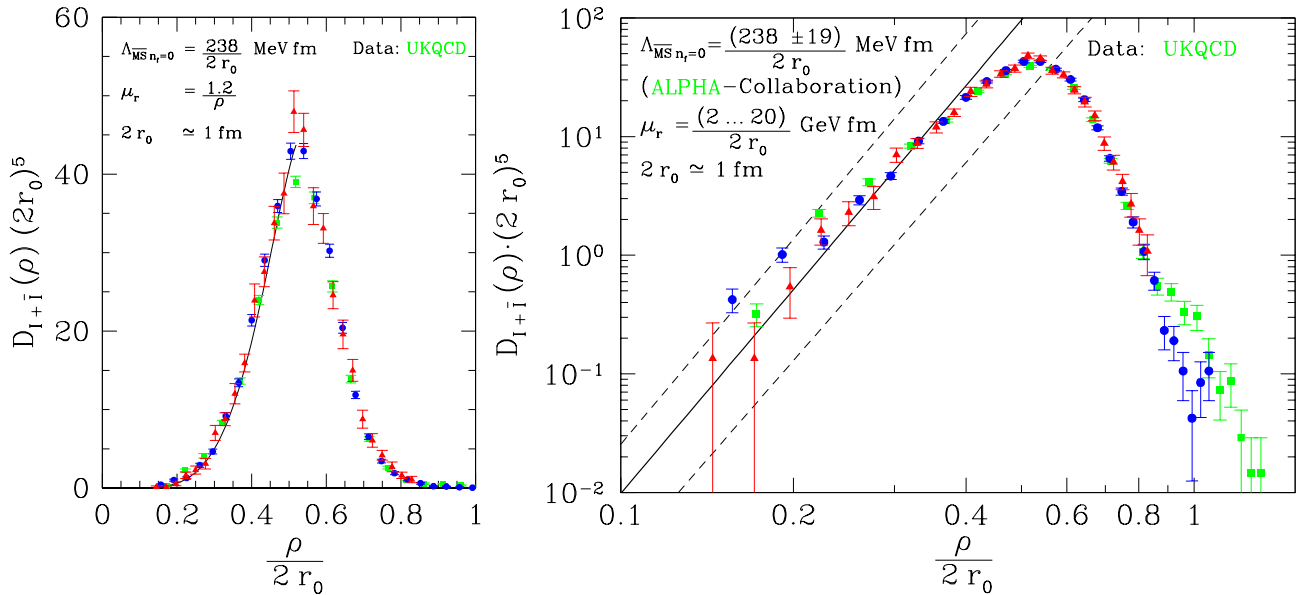


Figure 4: Continuum limit [14] of “equivalent” UKQCD data [23] for the $(I + \bar{I})$ -density at $(\beta, n_{\text{cools}}) = (6.0, 23)$ $[\square]$, $(6.2, 46)$ $[o]$, $(6.4, 80)$ $[\triangle]$. The striking agreement with $2D(\rho)$ of I -perturbation theory from (4) is apparent [14]. The 3-loop form of α_s with $\Lambda_{\overline{\text{MS}} n_f=0}$ from ALPHA [25] was used. (a) For $\mu_r = 1.2/\rho$, the agreement extends up to the peak; (b) Log-log plot to exhibit the expected power law $\sim \rho^6$ and the agreement in magnitude for small ρ over a wide range of μ_r . The dashed error band results from varying $\Lambda_{\overline{\text{MS}} n_f=0}$ and μ_r within its error and given range, respectively.

we have confirmed [23,14] the approximate validity of the dilute-gas picture for sufficiently *small* instantons² with $\rho \lesssim (0.3 - 0.5)$ fm. The latter results are based on the “packing fraction” [23] being < 1 and a test of the dilute-gas identity: $\langle Q^2 \rangle = N_{\text{tot}}$. Here Q is the topological charge and N_{tot} the total number of charges. These results strongly support the reliability of our calculations in DIS.

By means of the discussed saddle-point correspondence (5), these lattice constraints may be converted into a “fiducial” region for our cross-section predictions in DIS [9],

$$\left. \begin{array}{l} \rho^* \leq \rho_{\text{max}}^* \simeq 0.3 \text{ fm}; \\ \frac{R^*}{\rho^*} \geq \left(\frac{R^*}{\rho^*}\right)_{\text{min}} \simeq 1 \end{array} \right\} \Rightarrow \left\{ \begin{array}{l} Q' \geq Q'_{\text{min}} \simeq 8 \text{ GeV}; \\ x' \geq x'_{\text{min}} \simeq 0.35. \end{array} \right. \quad (6)$$

4 HERA cross-section

Figure 5 displays our finalized I -induced cross-section at HERA [9,10], as function of the cuts x'_{min} and Q'_{min} . For the minimal cuts (6) extracted from the UKQCD lattice simulation, we obtain

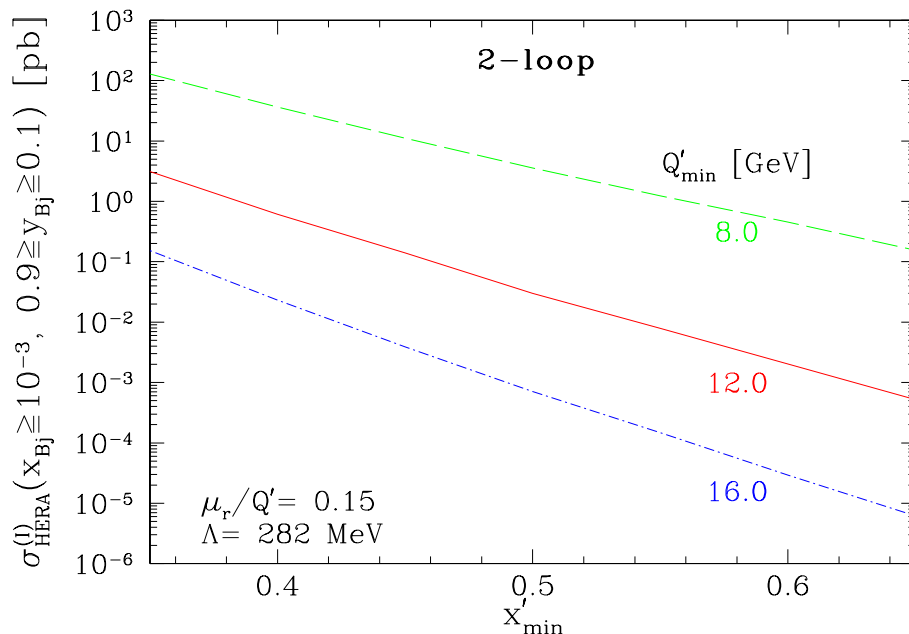


Figure 5: I -induced cross-section at HERA as function of the cuts in (x', Q') .

a surprisingly large cross-section,

$$\sigma_{\text{HERA}}^{(I)}(x' \geq 0.35, Q' \geq 8 \text{ GeV}) \simeq 126 \text{ pb}; \quad x_{\text{Bj}} \geq 10^{-3}; \quad 0.9 \geq y_{\text{Bj}} \geq 0.1. \quad (7)$$

Hence, with the total luminosity accumulated by experiments at HERA, $\mathcal{L} = \mathcal{O}(80) \text{ pb}^{-1}$, one already expects $\mathcal{O}(10^4)$ I -induced events on tape from this kinematical region. Note also that the cross-section quoted in Eq. (7) corresponds to a fraction of I -induced to normal DIS (nDIS) events of

$$f^{(I)} = \frac{\sigma_{\text{HERA}}^{(I)}}{\sigma_{\text{HERA}}^{(\text{nDIS})}} = \mathcal{O}(1) \%; \quad \text{for } x_{\text{Bj}} \geq 10^{-3}; \quad 0.9 \geq y_{\text{Bj}} \geq 0.1. \quad (8)$$

²Note that the full $(I + \bar{I})$ -ensemble without the size restriction is known *not* to be a dilute gas [23,21].

This is remarkably close to the published upper limits on the fraction of I -induced events [26], which are also on the one percent level.

There are still a number of significant uncertainties in our result for the cross-section. For *fixed* Q' and x' cuts, one of the dominant uncertainties arises from the experimental uncertainty in the QCD scale Λ . In the 2-loop expression for α_s with $n_f = 3$ (massless) flavours we used the value $\Lambda_{\overline{\text{MS}}}^{(3)} = 282$ MeV, corresponding to the central value of the DIS average for $n_f = 4$, $\Lambda_{\overline{\text{MS}}}^{(4)} = 234$ MeV [27]. If we change $\Lambda_{\overline{\text{MS}}}^{(3)}$ within the allowed range, $\approx \pm 65$ MeV, the cross-section (7) varies between 26 pb and 426 pb. Minor uncertainties are associated with the residual renormalization-scale dependence (c.f. figure 2) and the choice of the factorization scale. Upon varying the latter by an order of magnitude, the changes are in the $\mathcal{O}(20)$ % range only.

By far the dominant uncertainty in $\sigma_{\text{HERA}}^{(I)}$ arises, however, from the uncertainty in placing the (x', Q') cuts (c.f. figure 5). Hence, the constraints (6) from lattice simulations are extremely valuable for making concrete and reliable predictions of the I -induced rate at HERA.

5 Signatures and searches

An indispensable tool for investigating the structure of the I -induced final state and for developing optimized search strategies is our Monte-Carlo generator for I -induced DIS-events, QCDINS 1.60. Besides the matrix element for the I -induced hard subprocess, it provides leading-log parton showers and hadronization via its interface to HERWIG 5.9.

The characteristic features of the I -induced final state are illustrated in figure 6 (a) displaying the lego plot of a typical event from QCDINS 1.60 (c. f. also figure 1):

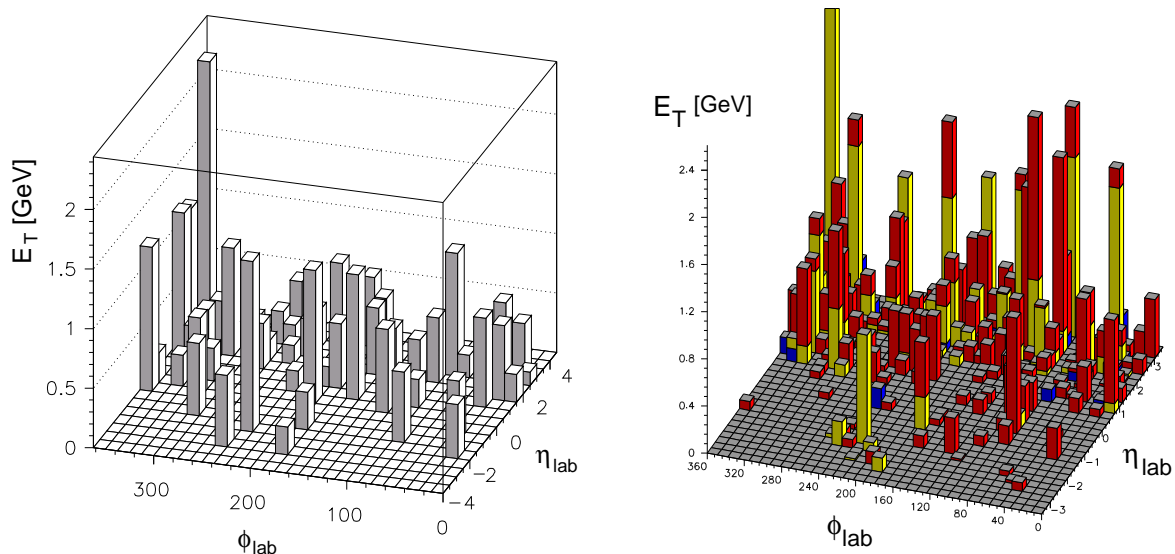


Figure 6: (a) Lego plot of a typical instanton-induced event from QCDINS 1.60.

(b) An interesting *real* “fireball” event in photoproduction from ZEUS [30] with very large total E_T and multiplicity.

Besides a single (not very hard) current-quark jet, one expects an accompanying densely populated “hadronic band”. For $x_{\text{Bj, min}} \simeq 10^{-3}$, say, it is centered around $\bar{\eta} \simeq 2$ and has a width of $\Delta\eta \simeq \pm 1$.

The band directly reflects the *isotropic* production of an I -induced “fireball” of $\mathcal{O}(10)$ partons in the I -rest system. Both the total transverse energy $\langle E_T \rangle \simeq 15$ GeV and the charged particle multiplicity $\langle n_c \rangle \simeq 13$ in the band are far higher than in normal DIS events. Finally, each I -induced event has to contain strangeness (and possibly also charm) such that the number of K^0 's amounts to $\simeq 2.2/\text{event}$.

Despite the high expected rate (7) of I -induced events at HERA, no *single* observable is known (yet) with sufficient nDIS rejection. Hence, a dedicated multi-observable analysis seems to be required. Neural network filters are being tried and exhibit a very good analyzing power if applied to $\gtrsim \mathcal{O}(5)$ observables [28]. Strategies to produce “instanton-enriched” data samples and to reconstruct (Q'^2, x') are under study and look quite promising [28]. Clearly, in all cases, a good understanding of the perturbative QCD background in the *tails* of the considered distributions is required.

6 Going beyond instanton-perturbation theory

A class of striking “fireball” events in photoproduction, with large total E_T and large multiplicity, has been reported [29] at this meeting (see e.g. figure 6 (b)). While the quantitative analysis is still in an early stage, these events seem to exhibit all characteristics of I -induced events (c.f. figure 6 (a)). However, it appears that – unlike ordinary QCD perturbation theory – the hard photoproduction limit, $Q^2 \Rightarrow 0$, $(E_T)_{\text{jet}}$ large, is not within the reach of strict I -perturbation theory. The reason is that in the $Q^2 \Rightarrow 0$ limit, we encounter a contribution to the photoproduction cross-section, which tends to *diverge*, if integrated over the I -size ρ . This IR divergence at large ρ is independent of the E_T of the (current quark) jet and directly associated with the “bad” large- ρ behaviour of the *perturbative* expression (4) for the I -density, $D(\rho) \sim \rho^{6-2/3n_f}$. In contrast, the *actual* form of $D(\rho)$ (c.f. figure 4) is strongly peaked around $\rho \simeq 0.5$ fm, and appears to *vanish* exponentially fast for larger ρ . The above “fireball” events and more generally, the ongoing I -searches at HERA, provide plenty of motivation for trying to extend our calculational framework beyond strict I -perturbation theory. We are thus led to make the following promising proposal in this direction:

One may try and replace the most strongly varying entries in the perturbative calculations, the I -density $D(\rho)$ and the $I\bar{I}$ -interaction $\Omega(R^2/(\rho\bar{\rho}), \dots)$, in (3), by their *actual* form as extracted from the recent non-perturbative lattice results [14].

The I -rates in photoproduction and the I -contributions to further interesting observables may then be calculated, and the (Q'^2, x') cuts in I -searches be considerably relaxed! Due to the strong peaking of $D(\rho)$, only the region around $\rho \simeq 0.5$ fm enters and the dilute-gas approximation may well continue to hold up to the peak (c.f. section 3).

References

- [1] A. Belavin, A. Polyakov, A. Schwarz and Yu. Tyupkin, *Phys. Lett. B* **59** (1975) 85.
- [2] T. Schäfer and E.V. Shuryak, *Rev. Mod. Phys.* **70** (1998) 323.
- [3] G. ‘t Hooft, *Phys. Rev. Lett.* **37** (1976) 8; *Phys. Rev. D* **14** (1976) 3432; *Phys. Rev. D* **18** (1978) 2199 (Erratum); *Phys. Rep.* **142** (1986) 357.

- [4] E. Witten, *Nucl. Phys. B* **156** (1979) 269;
G. Veneziano, *Nucl. Phys. B* **159** (1979) 213.
- [5] D. Diakonov, Lectures at the 1995 *Enrico Fermi School*, hep-ph/9602375.
- [6] I. Balitsky and V. Braun, *Phys. Lett. B* **314** (1993) 237.
- [7] A. Ringwald and F. Schrempp, hep-ph/9411217, in: *Quarks '94*, Proc. 8th Int. Seminar, Vladimir, Russia, 1994, eds. D. Gligoriev et al., pp. 170-193.
- [8] S. Moch, A. Ringwald and F. Schrempp, *Nucl. Phys. B* **507** (1997) 134.
- [9] A. Ringwald and F. Schrempp, hep-ph/9806528, *Phys. Lett. B* **438** (1998) 217.
- [10] S. Moch, A. Ringwald and F. Schrempp, to be published.
- [11] M. Gibbs, A. Ringwald and F. Schrempp, hep-ph/9506392, in: *Proc. Workshop on Deep Inelastic Scattering and QCD*, Paris, France, 1995, eds. J.-F. Laporte and Y. Sirois, pp. 341-344.
- [12] A. Ringwald and F. Schrempp, hep-ph/9610213, in: *Quarks '96*, Proc. 9th Int. Seminar, Yaroslavl, Russia, 1996, eds. V. Matveev *et al.*, Vol. I, pp. 29-54.
- [13] A. Ringwald and F. Schrempp, hep-ph/9706399, in: *Proc. 5th Int. Workshop on Deep Inelastic Scattering and QCD (DIS 97)*, Chicago, 1997, eds. J. Repond and D. Krakauer, pp. 781-786.
- [14] A. Ringwald and F. Schrempp, DESY 98-201.
- [15] C. Bernard, *Phys. Rev. D* **19** (1979) 3013;
A. Hasenfratz and P. Hasenfratz, *Nucl. Phys. B* **193** (1981) 210;
M. Lüscher, *Nucl. Phys. B* **205** (1982) 483.
- [16] T. Morris, D. Ross and C. Sachrajda, *Nucl. Phys. B* **255** (1985) 115.
- [17] P. Arnold and M. Mattis, *Phys. Rev. D* **44** (1991) 3650;
A. Mueller, *Nucl. Phys. B* **364** (1991) 109;
D. Diakonov and V. Petrov, in: *Proc. 26th LNPI Winter School*, (Leningrad, 1991), pp. 8-64.
- [18] A. Yung, *Nucl. Phys. B* **297** (1988) 47.
- [19] V.V. Khoze and A. Ringwald, *Phys. Lett. B* **259** (1991) 106.
- [20] J. Verbaarschot, *Nucl. Phys. B* **362** (1991) 33.
- [21] see e. g.:
P. van Baal, *Nucl. Phys. (Proc. Suppl.)* **63** (1998) 126;
J. Negele, hep-lat/9810053, Review at Lattice '98;
and references cited therein.
- [22] M.-C. Chu, J.M. Grandy, S. Huang and J.W. Negele, *Phys. Rev. D* **49** (1994) 6039.
- [23] D.A. Smith and M.J. Teper, (UKQCD Collab.), hep-lat/9801008, *Phys. Rev. D* **58** (1998) 014505 and M. Teper, private communication.

- [24] R. Sommer, hep-lat/9310022, *Nucl. Phys. B* **411** (1994) 839.
- [25] S. Capitani, M. Lüscher, R. Sommer and H. Wittig, (ALPHA Collab.), hep-lat/9810063, DESY 98-154.
- [26] S. Aid *et al.*, H1 Collaboration, *Nucl. Phys. B* **480** (1996) 3;
S. Aid *et al.*, H1 Collaboration, *Z. Phys. C* **72** (1996) 573;
T. Carli and M. Kuhlen, *Nucl. Phys. B* **511** (1998) 85.
- [27] Review of Particle Physics, Particle Data Group, *Phys. Rev. D* **54** (1996) 1.
- [28] T. Carli, private communication;
J. Gerigk, Diplome Thesis, DESY, Nov 1998, to be published.
- [29] Y. Yamazaki, talk in WG2/WG3 at this conference;
C. Nath, PhD thesis, Oxford 1998.
- [30] ZEUS Collaboration, event 38585, run 13990, 1995,
http://www-zeus.desy.de/~krakauer/disp/95_list.html.